Publishing Excellence
Inspiring Progress
ARISTON PUBLICATIONS
Quantum Advances
ISSN: 3143-0724 www.aristonpubs.com/journal/quantum-advances https://doi.org/10.69626/qa.2026.0077

RESEARCH ARTICLE

Inter – ring coupling effects on energy spectrum and thermodynamics in concentric double quantum rings

S. Sakiroglu[1], E. Kasapoglu[2], H. Sari[3*]

ABSTRACT: In this study, the dependence of the thermodynamic properties of a concentric double quantum ring system on geometric confinement parameters was investigated at different temperature values. The results show that the coupling between the rings and confinement strength play a dominant role in the energy spectrum and thermal response of the system. The mean energy and entropy exhibit a non-monotonic dependence on the inner radius, which is the result of the interplay between strong radial confinement and inter-ring coupling. Furthermore, it was concluded that the redistribution of energy levels depending on the strength of inter-ring coupling has a significant effect on the heat capacity behavior. In conclusion, the strong correlation between thermodynamic quantities and the energy spectrum, which is tunable with geometric confinement parameters, has significant implications for the design of nanoscale ring-based systems for thermal and quantum device applications.

Keywords: Quantum Ring; Thermal Properties; Geometric Confinement.

Received: 03 May 2026; Revised: 15 May 2026; Accepted: 30 May 2026; Published Online: 09 June 2026

1. INTRODUCTION

Concentric double quantum rings (CDQRs) are nanostructures consisting of two quantum rings that share the same center but have different radii. Like quantum dots (QDs), QRs have atom-like properties, making them suitable for potential applications in quantum computing and advanced photonics devices [1–7]. QRs have attracted intensive attention due to their unique multiply connected geometry, which makes them an intriguing subject of study. The electronic and optical properties of QRs are significantly affected by factors such as the inter-ring distance, geometry of the confinement potential, the coupling between the rings, and the applied external fields. These factors can lead to variations in energy levels and charge carrier dynamics, ultimately influencing the performance of devices based on these materials. Understanding these relationships is crucial for optimizing their applications in electronics and photonics. By applying external fields and adjusting the structural parameters, one can effectively tune both the electronic and optical properties of the system. These modifications lead to variations in the localization of charge carriers between the inner and outer rings, offering a powerful means to control the optical absorption and emission spectra as well as the dipole transition intensities. Some of the studies that theoretically investigated the effects of external fields on the electronic and optical properties of QR structures are [8–20]. Baghramyan et al. have studied the influence of an electric field on the electronic and absorption spectra in the CDQR. Furthermore, they have studied the effect of the direction of the incident

[1] Faculty of Science, Physics Department, Dokuz Eylül University, 35390 İzmir, Turkey.
[2] Sivas Cumhuriyet University, Science Faculty, Physics Department, 58140, Sivas, Turkey.
[3] Faculty of Education, Department of Mathematics and Natural Science Education, Sivas Cumhuriyet University, 58140 Sivas, Turkey.

* Author to whom correspondence should be addressed: sari@cumhuriyet.edu.tr (H. Sari)

© Ariston Publications 2026. All rights reserved.

light polarization on the absorption spectrum [8]. Culchac et al. investigated the effects of applied hydrostatic pressure and magnetic field on electron states and electron–heavy hole energy transitions in GaAs/GaAlAs CDQRs [9].

The effects of electric field, hydrostatic pressure, temperature, and aluminum concentration on the energy spectrum of CDQRs are calculated by Baghramyan et al. [10]. In [11], the electron and hole energies, as well as the far-infrared absorption spectra in the CDQW, were studied theoretically by varying the outer ring radius while keeping the inner ring radius fixed, under the magnetic field. In [12], the properties of the coupled CDQR system under an axial magnetic field and the effects of the coupling between the rings and the changing of the ring radii on the spectrum were investigated. Besides externally applied fields, the electronic and optical properties of CDQRs that have different confinement potentials in the presence and absence of hydrogen donor impurities have been intensively investigated [13–20]. As known, thermodynamic quantities such as average energy, specific heat, and entropy describe how charge carriers occupy available energy levels as temperature changes, and these quantities help determine how stable the quantum system is at different thermal conditions. Changes in these properties cause energy levels to rearrange in response to temperature or external fields. In this context, the thermodynamic properties of low-dimensional systems are also an interesting and important topic. Although extensive researches have been studied on the thermodynamic properties of quantum dots and/or quantum rings [21–26], to our knowledge no study has been conducted on the thermodynamic properties of CDQRs. So, in this study we aim to investigate the thermodynamic properties such as energy, entropy, mean energy and heat capacity of the GaAs CDQR.

2. THEORETICAL MODEL

In this study, we investigate the thermodynamic properties of a system composed of CDQRs. Two-dimensional contour map of the radial confinement potential of the CDQR is illustrated in Figure 1. The behavior of an electron confined within the CDQR is described by the two-dimensional Schrödinger equation given below:

$$\left[-\frac{\hbar^2}{2m^*}\nabla^2 + V(\rho)\right]\psi_i(\rho) = E_i\psi_i(\rho). \tag{1}$$

Here, m^* denotes the effective mass of the electron, and ∇^2 represents the Laplace operator. The geometric confining potential is defined as [13, 27]

$$V(\rho) = \frac{m^*\omega^2}{2}\min\left\{(\rho - R_1)^2, (\rho - R_2)^2\right\} \tag{2}$$

where $\rho = \sqrt{x^2 + y^2}$, R_1 and R_2 represent the inner and outer ring radii, respectively, while ω represents the harmonic oscillator frequency that describes the lateral confinement of electrons in each ring.

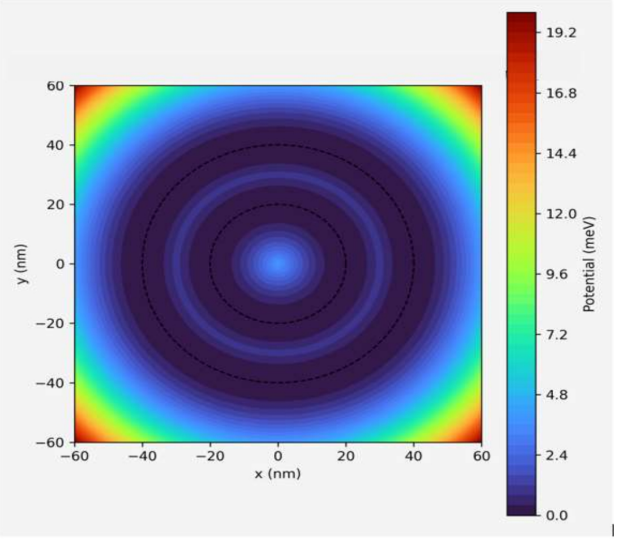

Fig. 1. Two-dimensional contour map of the radial confinement potential of the concentric double quantum ring (CDQR) for $R_1 = 20$ nm and $R_2 = 40$ nm with a confinement strength of $\hbar\omega = 20$ meV. The dashed circles indicate the equilibrium radii of the inner and outer quantum rings.

The two-dimensional diagonalization approach was utilized to determine the electron energy levels (E_i) and the corresponding eigenfunctions (ψ_i), as shown in [28, 29]. Within this framework, the electronic wave function is expanded in terms of a complete set of eigenfunctions of a two-dimensional infinite rectangular quantum well, according to

$$\psi_n(x,y) = \sum_{n_x,n_y} C_{n_x,n_y}\,\phi_{n_x,n_y}(x,y), \tag{3}$$

where C_{n_x,n_y} denote the expansion coefficients. The basis functions $\phi_{n_x,n_y}(x,y)$ are given by

$$\phi_{n_x,n_y}(x,y) = \frac{2}{\sqrt{L_xL_y}}\sin\left(\frac{n_x\pi x}{L_x} + \frac{n_x\pi}{2}\right) \times \sin\left(\frac{n_y\pi y}{L_y} + \frac{n_y\pi}{2}\right) \tag{4}$$

© Ariston Publications 2026. All rights reserved.

with L_x and L_y representing the widths of the confining potential in the x and y directions, respectively.

For numerical implementation, the basis set is truncated to 250 terms, which ensures rapid convergence and sufficient numerical accuracy. The Hamiltonian matrix constructed in this truncated basis is then diagonalized to obtain the energy spectrum and the corresponding eigenstates. All numerical computations presented in this study were performed using the Wolfram Mathematica software package [28, 29].

To evaluate the thermodynamic characteristics of a physical system, it is customary to model the system as energetically isolated except for thermal exchange with an external reservoir maintained at a fixed temperature T. Within the framework of the canonical ensemble, the statistical behavior of the system is fully characterized by its partition function, which can be written in the following form [28, 29]

$$Z = \sum_{i=0}^{\infty} e^{-\beta E_i}, \tag{5}$$

where

$$\beta = \frac{1}{k_B T},$$

k_B is the Boltzmann constant and discrete energy levels are described as E_i. The number of energy eigenstates used in the thermal analysis was chosen to satisfy the convergence condition for the highest temperature considered in this study, which is 300 K. Accordingly, a cutoff value consisting of 50 energy levels was adopted, which was proven to be sufficient to ensure the convergence of the calculated thermodynamic quantities across the entire range of system parameters examined.

The mean energy U of the CDQR is [30, 31]

$$U = k_B T^2 \frac{\partial}{\partial T} \ln Z. \tag{6}$$

The entropy of the system is

$$S = k_B \frac{\partial}{\partial T} (T \ln Z), \tag{7}$$

and the heat capacity is given as

$$C_V = k_B T \frac{\partial^2}{\partial T^2} (T \ln Z). \tag{8}$$

3. RESULTS AND DISCUSSION

The physical parameters adopted in the present calculations are as follows: the effective electron mass was taken as $m^* = 0.067 m_0$, where m_0 is the free-electron mass, and the outer ring radius was fixed at $R_2 = 40$ nm. The geometric dimensions of the concentric double quantum rings (CDQRs) were selected within experimentally reported ranges. Atomic force microscopy studies of InAs/GaAs and GaAs/AlGaAs heterostructures have demonstrated inner-ring radii between 10 and 25 nm, inter-ring barrier widths of 4-6 nm, and outer-ring radii extending up to 80-90 nm [32–34]. These experimentally realistic parameters ensure strong quantum confinement while preserving tunable coupling between the two rings. Likewise, the confinement strength $\hbar\omega$ was chosen within the experimentally accessible range of 10-40 meV reported for InAs/GaAs and GaAs/AlGaAs quantum-ring structures [33, 34].

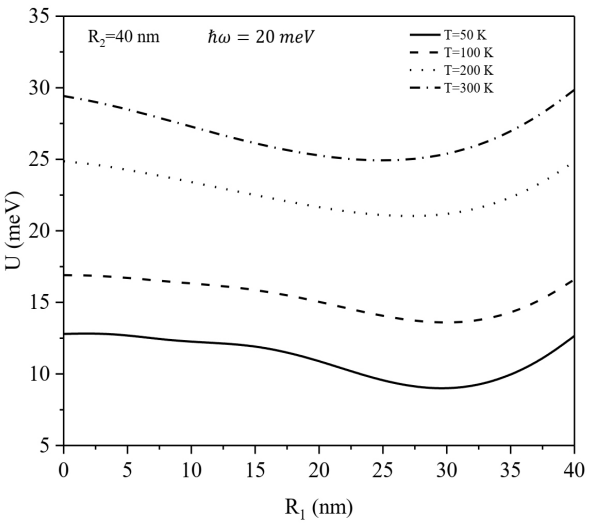

Fig. 2. For several temperature values, the variation of the mean energy U as a function of the inner ring radius R_1 of the CDQR.

Figure 2 shows the variation of the mean energy U of the CDQR system as a function of the inner-ring radius R_1 while keeping the outer-ring radius fixed at $R_2 = 40$ nm for several temperatures. The results demonstrate that both the confinement geometry and the electronic temperature strongly influence the energy spectrum. For all temperatures considered, the mean energy exhibits a non-monotonic dependence on R_1. At small values of R_1, strong radial confinement inside the inner ring increases the kinetic-energy contribution, leading to relatively high values of the mean energy. As R_1 increases,

© Ariston Publications 2026. All rights reserved.

the confinement weakens because the barrier separating the two rings becomes narrower, allowing greater spatial delocalization of the electronic wave functions and consequently reducing the mean energy. A minimum appears at approximately $R_1 \approx$ 25-30 nm, corresponding to an optimal balance between the confinement potentials of the inner and outer rings. Beyond this point, a further increase in R_1 weakens the effective coupling between the rings and shifts the electron localization toward the outer ring, resulting in an increase in the mean energy. Increasing the temperature produces an overall upward shift of the energy curves because thermal excitation populates higher-energy states, thereby increasing the ensemble-averaged energy. Nevertheless, the overall shape of the curves and the position of the minimum remain essentially unchanged, indicating that the energetically preferred radius is governed primarily by the confinement geometry rather than by temperature. Thus, temperature mainly modifies the occupation probabilities of the energy levels without significantly affecting the underlying spectrum.

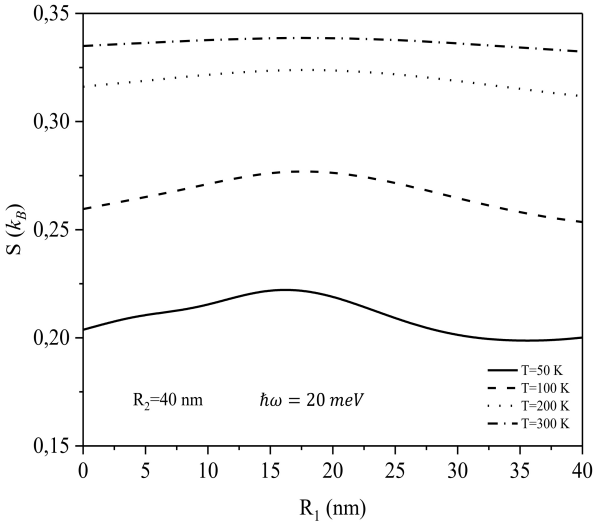

Fig. 3. The variation of the entropy S as a function of the inner ring radius R_1 of the CDQR for several temperatures.

Figure 3 presents the dependence of the entropy S on the inner-ring radius R_1 for several temperatures. As shown, the entropy exhibits broad maxima approximately at the same values of R_1 where the mean energy reaches its minimum. This inverse relationship between the mean energy and entropy arises because the system possesses a higher density of low-lying states and stronger level mixing near the energy minimum, thereby increasing the number of thermally accessible states. At small values of R_1, strong confinement shifts the energy levels upward and reduces their degeneracy, producing simultaneously higher mean energy and lower entropy. Conversely, at large values of R_1, the reduction of inter-ring coupling localizes carriers predominantly within the outer ring, limiting state mixing and again reducing the entropy while increasing the mean energy. Consequently, the entropy maximum naturally occurs in the geometric region where the electron wave functions are most effectively delocalized between the two rings.

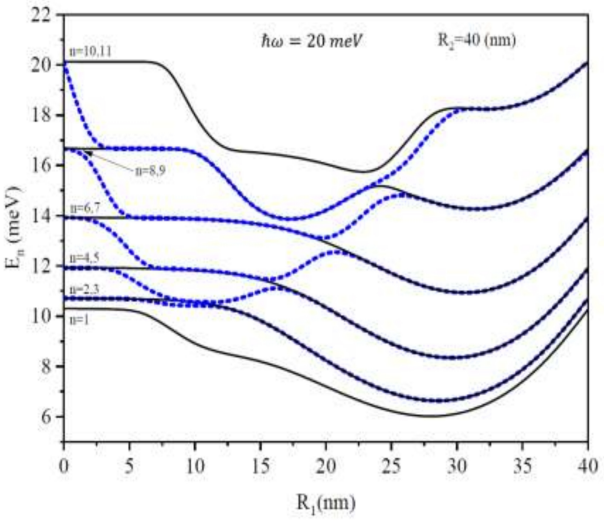

Fig. 4. Changes in the first eleven energy levels of the CDQR as a function of the inner ring radius R_1, for different temperatures.

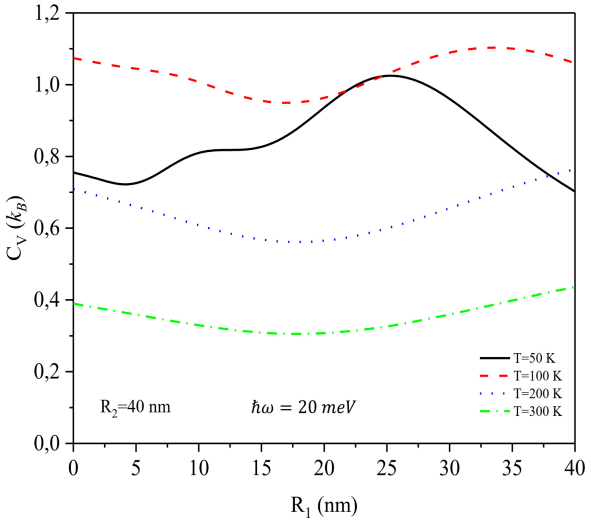

Fig. 5. The variation of the heat capacity C_V as a function of the inner ring radius R_1 of the CDQR for several temperatures.

Before analyzing the heat capacity, it is useful to examine the evolution of the electronic energy levels

 © Ariston Publications 2026. All rights reserved.

with the inner-ring radius because the heat capacity is highly sensitive to the energy-level distribution. Figure 4 illustrates the first eleven energy levels as functions of R_1. When $R_1 = 0$, the system behaves effectively as a quantum dot confined by the outer ring of radius R_2. As the inner-ring radius increases, the inner ring gradually forms, lifting the degeneracy of the energy levels owing to enhanced coupling between the inner and outer confinement regions. With a further increase in R_1, the separation between the two rings decreases and eventually disappears, transforming the structure into a single quantum ring with radius R_2. In this regime, the energy levels gradually converge and recover their degeneracy, producing an energy spectrum qualitatively similar to that observed at $R_1 = 0$. This redistribution of the energy spectrum has a pronounced influence on the thermal properties of the system, particularly on the heat capacity. Figure 5 presents the variation of the heat capacity C_V as a function of the inner-ring radius R_1 for different temperatures. Since the heat capacity is proportional to the temperature derivative of the mean energy, it is particularly sensitive to changes in the spacing between neighboring energy levels, as well as to level crossings and quasi-degenerate states in the low-energy spectrum. As illustrated in Figure 4, the electronic spectrum undergoes substantial restructuring as R_1 increases. The resulting reduction in the effective energy-level spacing enhances the sensitivity of the occupation probabilities to temperature, allowing relatively small thermal changes to redistribute electrons among nearby states. At low temperature ($T = 50$ K), only the lowest energy levels are thermally populated. As R_1 increases, particularly within the range $R_1 \approx$ 20-25 nm, the split excited states become nearly degenerate again, increasing the probability of thermal excitation and producing a pronounced maximum in the heat capacity. At larger values of R_1, the energy levels become more widely separated and ordered, reducing the number of thermally accessible states and causing the heat capacity to decrease. At $T = 100$ K, a larger number of low-energy states contributes to the thermal population, leading to broader and smoother variations of the heat capacity with R_1. A wide maximum appears around $R_1 \approx$ 30-35 nm, where the density of energy levels is relatively high. These results demonstrate that, at low temperatures, the heat capacity is governed primarily by the restructuring of the low-energy spectrum. At higher temperatures ($T = 200$ and 300 K), the heat capacity initially decreases with increasing R_1, reaches a minimum, and subsequently increases again. This behavior reflects the temperature-dependent changes in the density of states associated with the splitting and subsequent restoration of degeneracy of the excited energy levels as the inner-ring radius is varied.

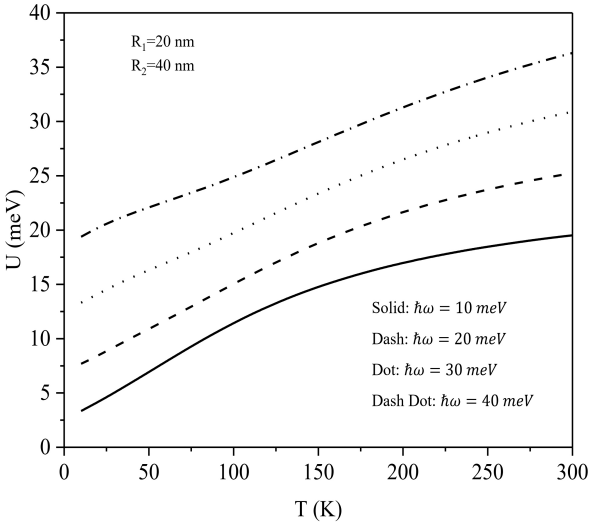

Fig. 6. The variation of the mean energy as function of the temperature, for several confinement strengths.

Figure 6 presents the temperature dependence of the mean energy U for a concentric double quantum ring with fixed radii $R_1 = 20$ nm and $R_2 = 40$ nm under different confinement strengths $\hbar\omega$. The results show that the mean energy increases monotonically with both temperature and confinement strength. At low temperatures, the electronic population is concentrated mainly in the ground state and a few low-lying excited states. Consequently, increasing the confinement strength shifts the entire energy spectrum toward higher energies owing to the larger quantization energy, resulting in higher values of the mean energy. As the temperature increases, progressively higher-energy states become thermally occupied, producing a continuous increase in U for all values of $\hbar\omega$. Because stronger confinement also increases the spacing between adjacent energy levels, the mean energy remains consistently higher throughout the investigated temperature range. These results demonstrate that the thermal behavior of the concentric double quantum ring can be effectively controlled by adjusting the strength of the geometric confinement. Figure 7 illustrates the temperature dependence of the entropy S for different confinement strengths. The entropy increases monotonically with temperature and exhibits a pronounced dependence on the confinement potential. At low temperatures, only the lowest electronic states are occupied, resulting in relatively small entropy. As the temperature rises, an increasing number of excited states become thermally accessible, broadening the occupation probability

© Ariston Publications 2026. All rights reserved.

distribution and producing a rapid increase in entropy. Increasing the confinement strength enlarges the separation between neighboring energy levels, thereby reducing the number of states that can be thermally populated at a given temperature. Consequently, the entropy decreases as $\hbar\omega$ increases. At sufficiently high temperatures, however, the entropy gradually approaches a saturation value for all confinement strengths. This behavior indicates that a large number of electronic states become occupied with nearly equal probabilities, reducing the influence of quantum confinement on the thermodynamic properties of the system.

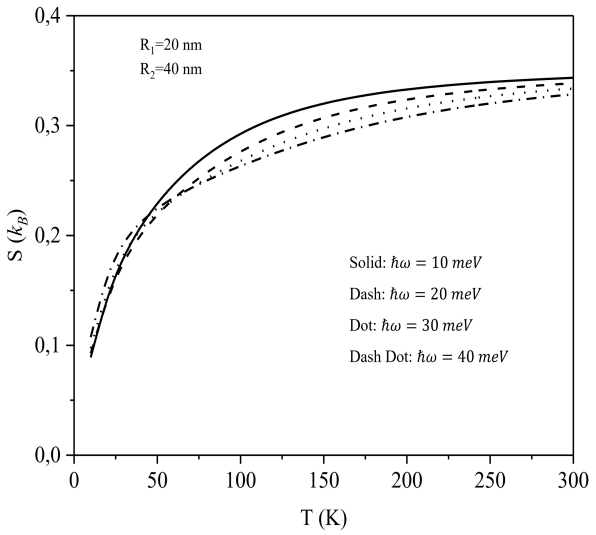

Fig. 7. Changes in the entropy as function of the temperature, for several confinement strengths.

Figure 8 shows the variation of the heat capacity C_V as a function of temperature for several values of the confinement strength. The results indicate that the heat capacity is strongly influenced by both temperature and the strength of the quantum confinement. At low temperatures, the heat capacity increases rapidly because thermal excitations occur primarily between the ground state and the first excited states. The pronounced peaks observed in this temperature region are characteristic of the Schottky anomaly, which arises from the effective two-level nature of the low-energy spectrum [35, 36]. This behavior is consistent with previous theoretical investigations of quantum-confined systems [35, 37]. In this regime, the thermal energy k_BT becomes comparable to the energy separation between the ground and first excited states, leading to a rapid redistribution of the electron population and producing a maximum in the heat capacity. The broad maximum observed at intermediate temperatures ($\sim$ 100--150 K) indicates the temperature range in which thermal occupation probabilities change most efficiently because the thermal energy is comparable to the characteristic level spacing. As discussed previously, increasing the confinement strength enlarges the separation between the quantized energy levels and consequently reduces the magnitude of the heat-capacity maximum.

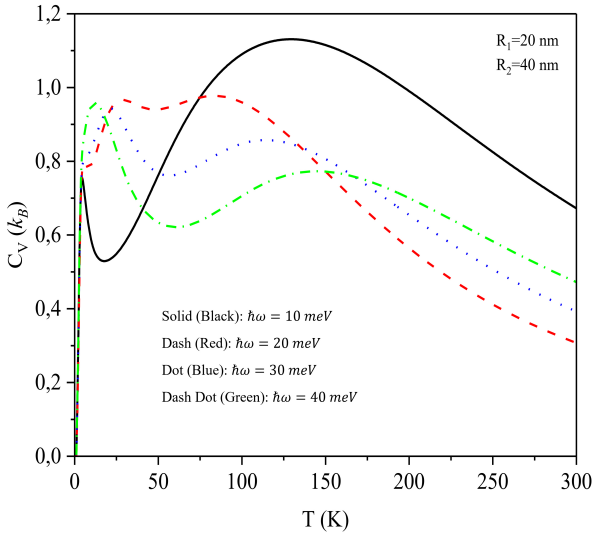

Fig. 8. The change of the heat capacity as function of the temperature, for several confinement strengths.

At higher temperatures, the heat capacity gradually decreases as the system approaches thermal saturation, where further increases in temperature produce only minor changes in the occupation probabilities of the available electronic states. These results clearly demonstrate that the heat capacity is governed by the discrete electronic spectrum and can be effectively tailored through the strength of the quantum confinement.

4. CONCLUSION

This study systematically investigated the thermodynamic properties of a concentric double quantum ring as a function of the temperature and confinement strength. The results show that the radius of the inner ring plays a key role in determining the energy spectrum, and consequently the mean energy, entropy and heat capacity of the system. The mean energy and entropy both exhibit pronounced non-monotonic dependencies on the inner radius, with characteristic extrema arising from the interplay between inner–outer ring coupling and the localization of carrier. A detailed examination of the low-energy levels reveals that the observed heat capacity behavior is directly

 © Ariston Publications 2026. All rights reserved.

governed by geometric confinement-dependent level splitting, quasi-degeneracy, and redistribution of the energy spectrum. At low temperatures, the heat capacity is highly sensitive to the redistribution of the energy spectrum, leading to distinct maxima and minima as the inner radius varies. At higher temperatures, this behaviour becomes smoother due to the increased contribution of excited states. In addition, it has been observed that the temperature-dependent heat capacity displays Schottky-type anomalies, the amplitude and position of which are governed by the confining strength. In conclusion, these results indicate that the thermal response of concentric double quantum rings can be effectively tuned through geometric design and confinement engineering. The strong correlation between energy spectrum and thermodynamic quantities has significant implications for the design of nanoscale ring-based systems for thermal and quantum device applications.

DECLARATIONS

Ethical Approval

We affirm that this manuscript is an original work, has not been previously published, and is not currently under consideration for publication in any other journal or conference proceedings. All authors have reviewed and approved the manuscript, and the order of authorship has been mutually agreed upon.

Funding

Funding not available

Availability of data and material

The datasets used and/or analyzed during the current study are available from the corresponding author on reasonable request.

Authors' contributions

S. Sakiroglu: Methodology, Writing, Formal analysis, Investigation; **E. Kasapoglu**: Writing, Formal analysis, Investigation; **H. Sari**: Formal analysis, Software, Investigation, Writing.

Conflicts of Interest

The authors declare that they have no financial or personal interests that could have influenced the research and findings presented in this paper. The authors alone are responsible for the content and writing of this article.

Data Availability

This manuscript has no associated data added to any data repository.

Acknowledgment

Not Applicable.

REFERENCES

[1] Chakraborty, T., **2003**. Quantum Dots: A Survey of the Properties of Artificial Atoms. *Advances in Solid State Physics*, 43, p.79-88.

[2] Suárez, F. and Granados, D. and Dotor, M. L. and García, J. M., **2004**. Vertical alignment and optical properties of self-assembled quantum rings. *Nanotechnology*, 15(4), p.S126-S130.

[3] Alén, B. and Martínez-Pastor, J. and Granados, D. and García, J. M., **2005**. Continuum and discrete excitation spectrum of single quantum rings. *Physical Review B*, 72(15), p.155331. https://doi.org/10.1103/PhysRevB.72.155331.

[4] Alén, B. and Bosch, J. and Granados, D. and Martínez-Pastor, J. and García, J. M. and González, L., **2007**. Oscillator strength reduction induced by external electric fields in self-assembled quantum dots and rings. *Physical Review B*, 75(4), p.045319. https://doi.org/10.1103/PhysRevB.75.045319.

[5] Huang, G. and Guo, W. and Bhattacharya, P. and Ariyawansa, G. and Perera, A. G. U., **2009**. A quantum ring terahertz detector with resonant tunnel barriers. *Applied Physics Letters*, 94(10), p.101115. https://doi.org/10.1063/1.3100407.

[6] Dai, J. H. and Lee, J. H. and Lin, Y. L. and Lee, S. C., **2008**. Optical characteristics of self-assembled quantum rings. *Japanese Journal of Applied Physics*, 47(4), p.2924-2927. https://doi.org/10.1143/JJAP.47.2924.

[7] Bhowmick, S. and Huang, G. and Guo, W. and Lee, C. S. and Bhattacharya, P. and Ariyawansa, G. and Perera, A. G. U., **2010**. Quantum ring infrared photodetectors with enhanced performance. *Applied Physics Letters*, 96(23), p.231103. https://doi.org/10.1063/1.3446857.

© Ariston Publications 2026. All rights reserved.

[8] Baghramyan, H. M. and Barseghyan, M. G. and Laroze, D. and Kirakosyan, A. A., **2016**. Electronic properties of semiconductor quantum rings under external fields. *Physica E: Low-dimensional Systems and Nanostructures*, 77, p.81-87. https://doi.org/10.1016/j.physe.2015.11.018.

[9] Culchac, F. and Porras-Montenegro, N. and Granada, J. and Latgé, A., **2008**. Electronic states in semiconductor quantum rings. *Microelectronics Journal*, 39(2), p.402-406. https://doi.org/10.1016/j.mejo.2007.08.022.

[10] Baghramyan, H. M. and Barseghyan, M. G. and Duque, C. A. and Kirakosyan, A. A., **2012**. Electronic and optical properties of semiconductor quantum rings. *Journal of Physics: Conference Series*, 350, p.012016. https://doi.org/10.1088/1742-6596/350/1/012016.

[11] Planelles, J. and Climente, J. I., **2005**. Electronic structure and optical properties of semiconductor quantum rings. *European Physical Journal B*, 48(1), p.65-71. https://doi.org/10.1140/epjb/e2005-00353-4.

[12] Fuster, G. and Pacheco, M. and Barticevic, Z., **2004**. Electronic properties of semiconductor quantum rings. *Brazilian Journal of Physics*, 34(2A), p.666-669. https://doi.org/10.1590/S0103-97332004000400028.

[13] Szafran, B. and Peeters, F. M., **2005**. Exciton states in semiconductor quantum rings. *Physical Review B*, 72(15), p.155316. https://doi.org/10.1103/PhysRevB.72.155316.

[14] Baghramyan, H. M. and Barseghyan, M. G. and Kirakosyan, A. A. and Restrepo, R. L. and Mora-Ramos, M. E. and Duque, C. A., **2014**. Electronic and optical properties of semiconductor quantum rings under external electric and magnetic fields. *Journal of Luminescence*, 145, p.676-682. https://doi.org/10.1016/j.jlumin.2013.08.043.

[15] Sherly, I. J. and Lidiya, A. E. and Nithiananthi, P., **2019**. Electronic and optical properties of semiconductor quantum rings under external perturbations. *Journal of Applied Physics*, 125(16), p.165707. https://doi.org/10.1063/1.5083153.

[16] Hahn, R. V. H. and Duque, C. A. and Mora-Ramos, M. E., **2025**. Magnetic-field effects on semiconductor quantum rings. *Physics Letters A*, 534, p.130226. https://doi.org/10.1016/j.physleta.2025.130226.

[17] Salehani, H. K., **2023**. Thermodynamic properties of semiconductor quantum rings under external fields. *Optical and Quantum Electronics*, 55, p.644. https://doi.org/10.1007/s11082-023-05071-0.

[18] Climente, J. I. and Planelles, J. and Barranco, M. and Malet, F. and Pi, M., **2006**. Electronic structure of semiconductor quantum rings. *Physical Review B*, 73(23), p.235327. https://doi.org/10.1103/PhysRevB.73.235327.

[19] Colletti, L. and Malet, F. and Pi, M. and Pederiva, F., **2009**. Many-electron effects in semiconductor quantum rings. *Physical Review B*, 79(12), p.125315. https://doi.org/10.1103/PhysRevB.79.125315.

[20] R-Fulla, M. and Marín, J. H. and Suaza, Y. A. and Duque, C. A. and Mora-Ramos, M. E., **2014**. Electronic and optical properties of semiconductor quantum rings in external fields. *Physics Letters A*, 378, p.2297-2303. https://doi.org/10.1016/j.physleta.2014.06.020.

[21] Sakiroglu, S. and Tuzemen, A. T. and Türk, G. E. and Sari, H., **2025**. Thermodynamic properties of semiconductor quantum rings under external electric and magnetic fields. *European Physical Journal Plus*, 140, p.143. https://doi.org/10.1140/epjp/s13360-025-05957-7.

[22] Khordad, R., **2013**. Thermodynamic properties of quantum ring systems under external magnetic field. *International Journal of Thermophysics*, 34, p.1148-1160. https://doi.org/10.1007/s10765-013-1452-8.

[23] Khordad, R., **2015**. Magnetic and thermodynamic properties of semiconductor quantum rings. *Modern Physics Letters B*, 29, p.1550137. https://doi.org/10.1142/S0217984915501377.

[24] Khordad, R. and Sedehi, H. R. R., **2018**. Thermodynamic properties of semiconductor quantum rings under hydrostatic pressure. *Journal of Low Temperature Physics*, 190, p.200-212. https://doi.org/10.1007/s10909-017-1838-5.

[25] Oliveira, R. R. S. and Araújo Filho, A. A. and Lima, F. C. E. and Maluf, R. V. and Almeida, C. A. S., **2019**. Thermodynamic properties of semiconductor quantum rings with Gaussian confinement. *European Physical Journal Plus*, 134, p.495. https://doi.org/10.1140/epjp/i2019-12837-6.

 © Ariston Publications 2026. All rights reserved.

[26] Lafaurie, L. G. and Suaza, Y. A. and Laroze, D. and Gutiérrez, W. and Marín, J. H., **2024**. Electronic and thermodynamic properties of semiconductor quantum rings under external fields. *Physica B: Condensed Matter*, 679, p.415786. https://doi.org/10.1016/j.physb.2024.415786.

[27] Malet, F. and Pi, M. and Barranco, M. and Lipparini, E., **2006**. Magnetic properties of interacting electrons in semiconductor quantum rings. *Physical Review B*, 74(19), p.193309. https://doi.org/10.1103/PhysRevB.74.193309.

[28] Tiutiunnyk, A. and Tulupenko, V. and Mora-Ramos, M. E. and Kasapoglu, E. and Ungan, F. and Sari, H. and Sokmen, I. and Duque, C. A., **2010**. Optical properties of semiconductor quantum rings under hydrostatic pressure. *Physics Letters A*, 374, p.3691-3696. https://doi.org/10.1016/j.physleta.2010.07.012.

[29] Sari, H. and Al, E. B. and Kasapoglu, E. and Sakiroglu, S. and Sokmen, I. and Toro-Escobar, M. and Duque, C. A., **2022**. Thermodynamic properties of cylindrical quantum rings under external electric and magnetic fields. *European Physical Journal Plus*, 137, p.464. https://doi.org/10.1140/epjp/s13360-022-02666-4.

[30] Hosseinpour, P., **2020**. The role of Rashba spin-orbit interaction and external fields in the thermal properties of a doped quantum dot with Gaussian impurity. *Physica B: Condensed Matter*, 593, p.412259. https://doi.org/10.1016/j.physb.2020.412259.

[31] Bhakti, B. and Datta, S. and Ghosh, M., **2024**. Electronic and optical properties of coupled quantum rings under external electric and magnetic fields. *Physica Status Solidi B*, 261, p.2300569. https://doi.org/10.1002/pssb.202300569.

[32] Mano, T. and others, **2005**. Self-assembly of concentric quantum double rings. *Nano Letters*, 5(3), p.425-428. https://doi.org/10.1021/nl048039m.

[33] Kuroda, T. and Mano, T. and Ochiai, T. and Sanguinetti, S. and Sakoda, K. and Kido, G. and Koguchi, N., **2005**. Optical transitions in self-assembled concentric quantum double rings. *Physical Review B*, 72(20), p.205301. https://doi.org/10.1103/PhysRevB.72.205301.

[34] Lorke, A. and Luyken, R. J. and Govorov, A. O. and Kotthaus, J. P. and Garcia, J. M. and Petroff, P. M., **2000**. Spectroscopy of nanoscopic semiconductor rings. *Physical Review Letters*, 84(10), p.2223-2226. https://doi.org/10.1103/PhysRevLett.84.2223.

[35] Rios-Alvarez, S. and Suaza, Y. A. and Marin, J. H., **2024**. Electronic and thermodynamic properties of coupled quantum rings under external perturbations. *Physica B: Condensed Matter*, 695, p.416553. https://doi.org/10.1016/j.physb.2024.416553.

[36] Tian, S. and Wu, Z., **2025**. Electronic and thermodynamic properties of semiconductor quantum rings under external magnetic fields. *Communications in Theoretical Physics*, 77, p.095502. https://doi.org/10.1088/1572-9494/ade5b2.

[37] Boyacioglu, B. and Chatterjee, A., **2012**. Electronic structure and magnetic properties of two-electron Gaussian quantum dots. *Journal of Applied Physics*, 112(8), p.083514. https://doi.org/10.1063/1.4759312.

© Ariston Publications 2026. All rights reserved.